

NeRF-SOS: ANY-VIEW SELF-SUPERVISED OBJECT SEGMENTATION ON COMPLEX SCENES

Zhiwen Fan¹, Peihao Wang¹, Xinyu Gong¹, Yifan Jiang¹, Dejie Xu¹, Zhangyang Wang¹

¹University of Texas at Austin

{zhiwenfan, atlaswang}@utexas.edu

ABSTRACT

Neural volumetric representations have shown the potential that Multi-layer Perceptrons (MLPs) can be optimized with multi-view calibrated images to represent scene geometry and appearance, without explicit 3D supervision. Object segmentation can enrich many downstream applications based on the learned radiance field. However, introducing hand-crafted segmentation to define regions of interest in a complex real-world scene is non-trivial and expensive as it acquires per view annotation. This paper carries out the exploration of self-supervised learning for object segmentation using NeRF for complex real-world scenes. Our framework, called *NeRF with Self-supervised Object Segmentation (NeRF-SOS)*, couples object segmentation and neural radiance field to segment objects in any view within a scene. By proposing a novel collaborative contrastive loss in both appearance and geometry levels, NeRF-SOS encourages NeRF models to distill compact geometry-aware segmentation clusters from their density fields and the self-supervised pre-trained 2D visual features. The self-supervised object segmentation framework can be applied to various NeRF models that both lead to photo-realistic rendering results and convincing segmentation maps for both indoor and outdoor scenarios. Extensive results on the *LLFF*, *Tank & Temple*, and *BlendedMVS* datasets validate the effectiveness of NeRF-SOS. It consistently surpasses other 2D-based self-supervised baselines and predicts finer semantics masks than existing supervised counterparts. Code is available at: <https://github.com/VITA-Group/NeRF-SOS>.

1 INTRODUCTION

Modeling the geometry of a scene is fundamental to computation vision. For example, portable Augmented Reality (AR) devices (e.g., the Magic Leap One) reconstruct the scene geometry and further localize users (DeChicchis, 2020). However, despite the geometry, it hardly understands the surrounding objects in the scene, and thus meets difficulty when enabling interaction between humans and environments. The hurdles of understanding and segmenting the surrounding objects can be mitigated by collecting human-annotated data from diverse environments, but that could be difficult in practice due to the costly labeling procedure. Therefore, there has been growing interest to build an intelligent geometry modeling framework without heavy and expensive annotations.

Recently, neural volumetric rendering techniques show great power on scene reconstruction. Especially, neural radiance field (NeRF) and its variants (Mildenhall et al., 2020a; Zhang et al., 2020; Barron et al., 2021) adopt multi-layer perceptrons (MLPs) to learn continuous representation and utilize calibrated multi-view images to render unseen views with fine-grained details. Besides rendering quality, the ability of scene understanding has been explored by several recent works (Vora et al., 2021; Yang et al., 2021; Zhi et al., 2021). Nevertheless, they either require dense view annotations to train a heavy 3D backbone for capturing semantic representations (Vora et al., 2021; Yang et al., 2021), or necessitate human intervention to provide sparse semantic labels (Zhi et al., 2021). Recent self-supervised object discovery approaches on neural radiance fields (Yu et al., 2021c; Vora et al., 2021; Stelzner et al., 2021) tries to decompose objects from givens scenes on the synthetic indoor data, however, still remains a gap to be applied in complex real-world scenarios.

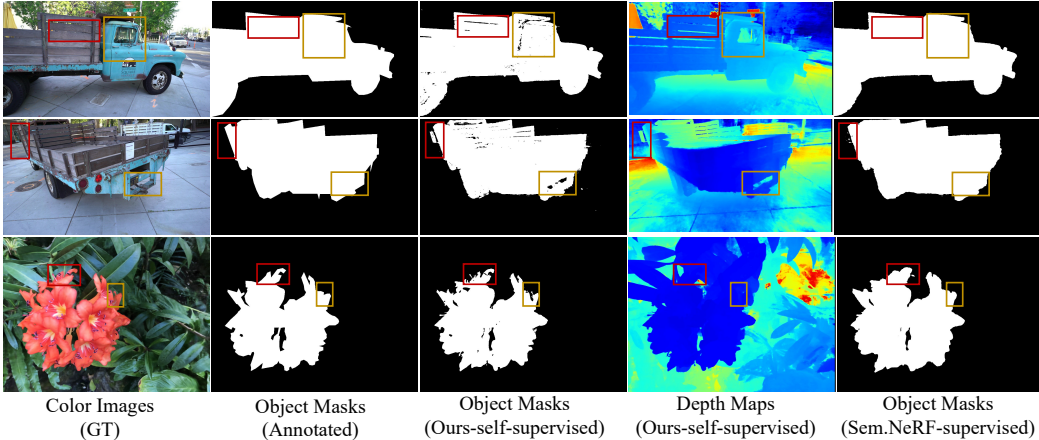


Figure 1: **Visual examples.** From left to right: ground truth color images, annotated object masks, object masks rendered by NeRF-SOS, depth maps rendered by NeRF-SOS, and object masks rendered by Semantic-NeRF (Zhi et al., 2021), respectively. Compared to the previous methods, NeRF-SOS generates faithful object masks with finer local details.

In contrast to previous works, we take one leap further to investigate a more general setting, to segment 3D objects in real-world scenes using general NeRF models. Driven by this motivation, we design a new self-supervised object segmentation framework for NeRF using a collaborative contrastive loss: adopting features from a self-supervised pre-trained 2D backbone (“**appearance level**”) and distilling knowledge from the geometry cues of a scene using the density field of NeRF representations (“**geometry level**”). To be more concrete, we learn from a pre-trained 2D feature extractor in a self-supervised manner (e.g., DINO (Caron et al., 2021)), and inject the visual correlations across views to form distinct feature clusters under NeRF formulation. We seek a geometry-level contrastive loss by formulating a geometric correlation volume between NeRF’s density field and the segmentation clusters to make the learned feature clusters aware of scene geometry. The proposed self-supervised object segmentation framework tailored for NeRF, dubbed **NeRF-SOS**, acts as a general implicit framework and can be applied to any existing NeRF models with end-to-end training. We implement and evaluate NeRF-SOS, using vanilla NeRF (Mildenhall et al., 2020a) for real-world forward-facing scenes (*Fortress* and *Flower*) and object-centric scenes (BlendedMVS (Yao et al., 2020)); and using NeRF++ (Zhang et al., 2020) for outdoor unbounded scene (*Truck*). Experiments show that NeRF-SOS significantly outperforms state-of-the-art 2D object discovery methods and by producing view-consistent segmentation clusters: a few examples are shown in Figure 1.

We summarize the main contributions as follows:

- We explore how to effectively apply the self-supervised learned 2D visual feature for 3D representations via an appearance contrastive loss, which forms compact feature clusters for any-view object segmentation in complex real-world scenes.
- We propose a new geometry contrastive loss for object segmentation. By leveraging its density field, our proposed framework can further inject scene geometry into the segmentation field, making the learned segmentation clusters geometry-aware.
- The proposed collaborative contrastive framework can be implemented upon NeRF and NeRF++, for indoor and unbounded real-world scenarios. Experiments show that our self-supervised object segmentation quality consistently surpasses 2D object discovery methods and yields finer-grained segmentation results than supervised counterparts (Zhi et al., 2021).

2 RELATED WORK

Neural Radiance Fields Neural Radiance Fields (NeRF) is first proposed by Mildenhall *et al.* (Mildenhall et al., 2020b), which models the underlying 3D scenes as continuous volumetric fields of color and density via layers of MLP. The input of a NeRF is a 5D vector, containing a 3D location (x, y, z) and a 2D viewing direction (θ, ϕ) . Owing to NeRF’s representation power and it

does not require explicit geometry used to guide the training, several following works emerge trying to address its limitations and improve the performance, such as fast training (Sun et al., 2021; Deng et al., 2021), efficient inference (Rebain et al., 2020; Liu et al., 2020a; Lindell et al., 2020; Garbin et al., 2021; Reiser et al., 2021; Yu et al., 2021a; Lombardi et al., 2021), better generalization (Schwarz et al., 2020a; Trevithick & Yang, 2020; Wang et al., 2021b; Chan et al., 2020; Yu et al., 2021b; Johari et al., 2021), supporting unconstrained scene (Martin-Brualla et al., 2020; Chen et al., 2021), editing (Liu et al., 2021; Jiakai et al., 2021; Wang et al., 2021a; Jang & Agapito, 2021), multi-task learning (Zhi et al., 2021) and view synthesis for unbounded scenes (Zhang et al., 2020; Barron et al., 2021). In this paper, we treat NeRF as a powerful implicit scene representation and study how to segment objects from a complex real-world scene without any supervision.

Self-supervised 2D Image Segmentation Techniques in self-supervised feature learning (Chen et al., 2020) by maximizing mutual information between an image and its augmentation can be used for self-supervised segmentation (Ji et al., 2019). Successive works (Li et al., 2021; Van Gansbeke et al., 2020; Cho et al., 2021; Hwang et al., 2019) either improve the clustering process or adopts Expectation-Maximization to refine segmentation. MaskContrast (Van Gansbeke et al., 2021) achieves better results by contrasting learned features within and across the saliency masks, and STEGO (Hamilton et al., 2022) utilizes a more powerful pre-trained model DINO-ViT (Caron et al., 2021) and constructs image feature correspondence for contrastive learning. IEM (Savarese et al., 2021) proposes to partition images into maximally independent sets. These methods perform well on 2D image pairs. However, it is non-trivial to implement self-supervised 2D segmentation upon neural radiance field due to the following reasons: **1).** self-supervised 2D methods failed to consider 3D view consistency. **2).** self-supervised 2D image-based methods work on an entire image which is prohibitive for NeRF since NeRF can only render a small patch each time due to the limitation of the volume rendering process (Drebin et al., 1988).

Object Co-segmentation without Explicit Learning Our work aims to discover and segment visually similar objects in the radiance field and, therefore, can render novel views with object masks. It is close to the object co-segmentation (Rother et al., 2006) which aims to segment the common objects from a set of images (Li et al., 2018). Object co-segmentation has been widely adopted in computer vision and computer graphics applications, including browsing in photo collections (Rother et al., 2006), 3D reconstruction (Kowdle et al., 2010), semantic segmentation (Shen et al., 2017), interactive image segmentation (Rother et al., 2006), object-based image retrieval (Vicente et al., 2011), and video object tracking/segmentation (Rother et al., 2006). (Rother et al., 2006) first shows that segmenting two images outperforms the independent counterpart. This idea is analogous to the contrastive learning way in later approaches. Especially, the authors in (Hénaff et al., 2022) propose the self-supervised segmentation framework using object discovery networks. (Siméoni et al., 2021) localizes the objects with a self-supervised transformer. (Hamilton et al., 2022) introduces the feature correspondences that distinguish between different classes. Most recently, a new co-segmentation framework based on DINO feature (Amir et al., 2021) has been proposed and achieves better results on object co-segmentation and part co-segmentation.

However, extending 2D object discovery to NeRF is non-trivial as they cannot learn the geometric cues in multi-view images. uORF (Yu et al., 2021c) and ObSuRF (Stelzner et al., 2021) use slot-based CNN encoders and object-centric latent codes for unsupervised 3D scene decomposition. Although they enable unsupervised 3D scene segmentation and novel view synthesis, experiments are on synthetic datasets, leaving a gap for complex real-world applications. Besides, a Gated Recurrent Unit (GRU) and multiple NeRF models are used, making the framework difficult to be applied to other NeRF models. Most recently, Kobayashi et al. (2022) propose to distill the visual feature from supervised CLIP-LSeg or self-supervised DINO into a 3D feature field, via an element-wise feature distance loss function. It can discover the object using a query text prompt or a patch. In contrast, we design a new collaborative contrastive loss on both appearance and geometry levels, to find the objects with a similar appearance and location. Owing to the formulation, we can distill the rich 2D visual representations and their scene geometry into compact geometry-aware segmentation clusters. The collaborative design is general and can be plug-and-play to different NeRF models.

3 METHOD

Overview We show how to extend existing NeRF models to segment objects in both training and inference. As seen in Figure 2, we augment NeRF models by appending a parallel segmentation branch to predict point-wise implicit segmentation feature s . Pixel-wise feature field is obtained

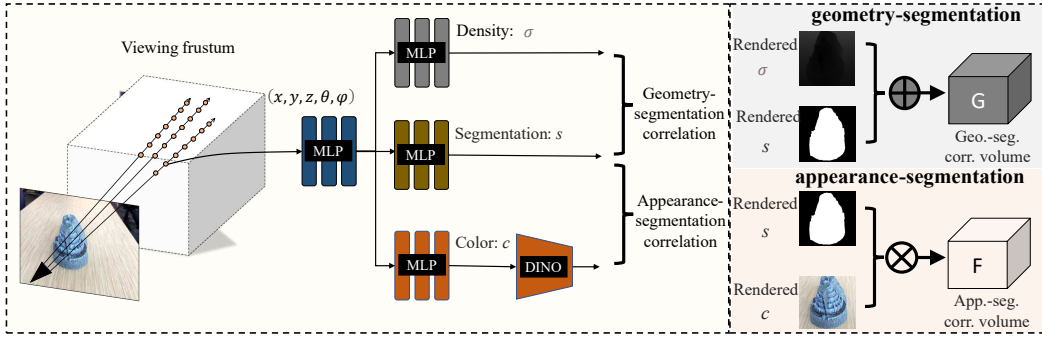


Figure 2: **The overall pipeline of the proposed NeRF-SOS.** Input with rays cast from multiple views, we render the corresponding color patch (c), segmentation patch (s), and depth patch (σ). Then, appearance-segmentation correlations and geometry-segmentation correlations are used to formulate a collaborative contrastive loss, enabling NeRF-SOS to render object masks from any viewpoint using the distilled segmentation field.

via volume rendering (Drebin et al., 1988) along each ray. We propose to update the segmentation feature field using a collaborative loss in both appearance and geometry levels. During inference, a clustering operation (e.g., K-means) is used to generate object masks, based on the rendered feature field. Specifically, inputs with multiple rays cast from several cameras, NeRF-SOS can render the depth σ , segmentation s , and color c . Next, we fed the rendered color patch c into a self-supervised pre-trained framework (e.g., DINO-ViT (Caron et al., 2021)) to generate feature tensor f , constructing appearance-segmentation correlation volume between f and s . Similarly, a geometry-segmentation correlation volume is instantiated using σ and s . By formulating positive/negative pairs from different views, we can distill the correlation pattern in both visual feature and scene geometry into the compact segmentation field s .

3.1 PRELIMINARIES

Neural Radiance Fields NeRF represents 3D scenes as radiance fields, where each point has a value of color and density. Such a radiance field can be formulated as $F : (\mathbf{x}, \boldsymbol{\theta}) \mapsto (\mathbf{c}, \sigma)$, where $\mathbf{x} \in \mathbb{R}^3$ is the spatial coordinate, $\boldsymbol{\theta} \in [-\pi, \pi]^2$ denotes the viewing direction, and $\mathbf{c} \in \mathbb{R}^3, \sigma \in \mathbb{R}_+$ represent the RGB color and density, respectively. NeRF reconstructs a radiance field by representing this 5D vector-valued function as a coordinate-based neural network Tancik et al. (2020), and optimizing it to make its multi-view rendering satisfy the captured images. Such neural network is composed of a Positional Embedding (PE) layer (Tancik et al., 2020) and an Multi-Layer Perceptron (MLP): $F = \gamma \circ \text{MLP}$. To form an image, NeRF traces a ray $\mathbf{r} = (\mathbf{o}, \mathbf{d}, \boldsymbol{\theta})$ for each pixel on the image plane, where $\mathbf{o} \in \mathbb{R}^3$ denotes the position of the camera, $\mathbf{d} \in \mathbb{R}^3$ is the direction of the ray, and $\boldsymbol{\theta} \in [-\pi, \pi]^2$ is the angular viewing direction. Afterwards, NeRF evenly samples K points $\{t_i\}_{i=1}^K$ between the near-far bound $[t_n, t_f]$ along the ray. Then, NeRF adopts volumetric rendering and numerically evaluates the ray integration (Max, 1995) by the quadrature rule:

$$\mathbf{C}(\mathbf{r}) = \sum_{k=1}^K T(k)(1 - \exp(-\sigma_k \delta t_k)) \mathbf{c}_k \quad \text{where } T(k) = \exp\left(-\sum_{l=1}^{k-1} \sigma_l \delta t_l\right), \quad (1)$$

where $\delta_k = t_{k+1} - t_k$ are intervals between sampled points, and $(\mathbf{c}_k, \sigma_k) = F(\mathbf{o} + t_k \mathbf{d}, \boldsymbol{\theta})$ are output from the neural network. With this forward model, NeRF optimizes the photometric loss between rendered ray colors and ground-truth pixel colors defined as follows:

$$\mathcal{L}_{\text{photometric}} = \sum_{(\mathbf{r}, \hat{\mathbf{C}}) \in \mathcal{R}} \left\| \mathbf{C}(\mathbf{r}) - \hat{\mathbf{C}} \right\|_2^2, \quad (2)$$

where \mathcal{R} defines a dataset collecting all pairs of ray and ground-truth colors from captured images.

Self-supervised Learned 2D Representations DINO-ViT (Caron et al., 2021) largely simplifies self-supervised learning by applying a knowledge distillation paradigm (Hinton et al., 2015) with a momentum encoder (He et al., 2020), where the model is simply updated by a cross-entropy loss.

Recent works (Amir et al., 2021; Hamilton et al., 2022) leverage DINO as a powerful feature extractor and proves it can learn feature correspondence for image pairs. Although DINO stands for a promising self-supervised pre-trained model with rich representations, the challenge still exists in how to leverage 2D representation to help scene understanding in the neural radiance field.

3.2 CROSS VIEW APPEARANCE CORRESPONDENCE

Semantic Correspondence across Views Tremendous works have explored and demonstrated the importance of object appearance when generating compact feature correspondence across views (Hénaff et al., 2022; Li et al., 2018). This peculiarity is then utilized in self-supervised 2D semantic segmentation frameworks (Hénaff et al., 2022; Li et al., 2018; Chen et al., 2020) to generate semantic representations by selecting positive and negative pairs with either random or KNN-based rules (Hamilton et al., 2022). Drawing inspiration from these prior arts, we construct the visual feature correspondence for NeRF at the appearance using a heuristic rule. To be more specific, we leverage the self-supervised model (e.g., DINO-ViT (Caron et al., 2021)) learned from 2D image sets to distill the rich representations into compact and distinct segmentation clusters. More formally, we introduce a four-layer MLP to segment objects in the radiance field parallel to the density branch and appearance branch of NeRF models (Mildenhall et al., 2020a). Inputting the camera origin and ray cast directions, we first render multiple image patches from various viewpoints using Equation 1, then we resize them to 224×224 and feed them into DINO-ViT. The generated feature tensors from DINO are of $H' \times W' \times C'$ as their spatial dimensions. They are then used to generate the appearance correspondence volume (Teed & Deng, 2020; Hamilton et al., 2022) across views, to measure the similarity between two regions of different views:

$$F_{hwh'w'} := \sum_c \frac{f_{chw} f'_{ch'w'}}{|f_{hw}| |f'_{h'w'}|}, \quad (3)$$

where f and f' stand for the extracted DINO feature from two random patches in different views, (h, w) and (h', w') denote the spatial location on feature tensor for f and f' , respectively, and the c traverses through the feature channel dimension.

Distilling Semantic Correspondence into Segmentation Field

The correspondence volume F from DINO has been verified it has the potential to effectively recall true label co-occurrence from image collections (Hamilton et al., 2022). We next explore how to learn a segmentation field s by leveraging F . Inspired by CRF and STEGO (Hamilton et al., 2022) where they refine the initial predictions using color or feature-correlated regions in the 2D image. We propose to append an extra segmentation branch to predict segmentation field, formulating segmentation correspondence volume by leveraging its predicted segmentation logits using the same rule with Equation 3. Then, we construct the appearance-segmentation correlation aims to enforce the elements of s and s' closer if f and f' are tightly coupled, where the expression with and without the superscript indicates two different views. The volume correlation can be achieved via an element-wise multiplication between S and F , and thereby, we have the appearance contrastive loss \mathcal{L}_{app} :

$$\mathcal{C}_{app}(\mathbf{r}, b) := - \sum_{hwh'w'} (F_{hwh'w'} - b) S_{hwh'w'} \quad (4)$$

$$\mathcal{L}_{app} = \lambda_{id} \mathcal{C}_{app}(\mathbf{r}_{id}, b_{id}) + \lambda_{neg} \mathcal{C}_{app}(\mathbf{r}_{neg}, b_{neg}) \quad (5)$$

where $S_{hwh'w'} := \sum_c \frac{s_{chw} s'_{ch'w'}}{|s_{hw}| |s'_{h'w'}|}$ indicates the segmentation correspondence volume between two views, \mathbf{r} is the cast ray fed into NeRF, b is a hyper-parameter to control the positive and negative pressure. λ_{id} and λ_{neg} indicate loss force between identity pairs (positive) and distinct pairs (negative). The intuition behind the above equation is that minimizing \mathcal{L}_{app} with respect to S , to enforce entries in segmentation field s to be large when $F - b$ are positive items and pushes entries to be small if $F - b$ are negative items.

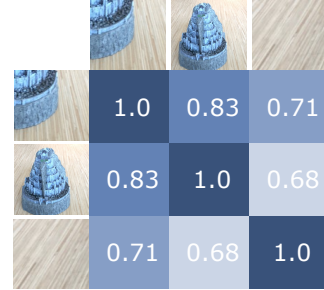


Figure 3: Different patches rendered by NeRF. The scores are computed by mutual cosine similarities of [CLS] tokens.

Discover Patch Relationships To effectively find the positive/negative pairs for the construction of Equation 5, we compute a similarity matrix based on the extracted [CLS] token from DINO-ViT, with the rendered image patches from \mathbf{c} as input. The score is calculated by the cosine similarity between arbitrary patches, resulting in a $N \times N$ symmetric lookup table, for N input patches. We obtain N positive pairs by the diagonal entries, and N negative pairs by finding the lowest score in each row. An example using three patches from different views is shown in Figure 3. We find [CLS] token captures a high-level semantic appearance after self-supervised pre-training (Tumanyan et al., 2022) and it can effectively discover patches’ similarities within our end-to-end optimization process.

3.3 CROSS VIEW GEOMETRY CORRESPONDENCE

Geometry Correspondence across Views With the appearance level distillation from the DINO feature to the low-dimensional segmentation embedding in the segmentation field s , we can successfully distinguish the salient object with a similar appearance. However, s may mistakenly cluster different objects together, as s may be obfuscated by objects with distinct spatial locations but similar appearances. To solve this problem, we propose to leverage the density field that already exists in NeRF models to formulate a new geometry contrastive loss. Specifically, given a batch of M cast ray \mathbf{r} as NeRF’s input, we can obtain the density field of size $M \times K$ where K indicates the number of sampled points along each ray. By accumulating the discrete bins along each ray, we can roughly represent the density field as a single 3D point:

$$\mathbf{p} = \mathbf{r}_o + \mathbf{r}_d \cdot D \quad (6)$$

$$D(\mathbf{r}|\Theta) = \sum_{k=1}^K T(k)(1 - \exp(-\sigma_k \Delta t_k))t_k \quad (7)$$

where \mathbf{p} is the accumulated 3D point along the ray, D is the estimated depth value of the corresponding pixel index. Inspired by Point Transformer (Zhao et al., 2021) which uses point-wise distance as representation, we utilize the estimated point position as a geometry cue to formulate a new geometry level correspondence volume across views by measuring point-wise absolute distance:

$$G_{hwh'w'} := \sum_c \frac{1}{|g_{chw} - g'_{ch'w'}| + \epsilon} \quad (8)$$

where g and g' are the estimated 3D point positions in two random patches of different views, (h, w) and (h', w') denote the spatial location on feature tensor for g and g' , respectively.

Injecting Geometry Coherence into Segmentation Field To inject the geometry cue from the density field to the segmentation field, we formulate segmentation correspondence volume S and geometric correspondence volume G using the same rule of Equation 4. By pulling/pushing positive/negative pairs, we come up with a new geometry-aware contrastive loss \mathcal{L}_{geo} using G and S :

$$\mathcal{C}_{geo}(\mathbf{r}, b) := - \sum_{hwh'w'} (G_{hwh'w'} - b)S_{hwh'w'} \quad (9)$$

$$\mathcal{L}_{geo} = \lambda_{id}\mathcal{C}_{geo}(\mathbf{r}_{id}, b_{id}) + \lambda_{neg}\mathcal{C}_{geo}(\mathbf{r}_{neg}, b_{neg}) \quad (10)$$

Same as appearance contrastive loss, we find identity (positive) pairs and negative pairs via the pair-wise cosine similarity of [CLS] tokens.

3.4 OPTIMIZING WITH STRIDE RAY SAMPLING

Neural radiance field casts a number of rays (typically not adjacent) from the camera origin, intersecting the pixel, to generate input 3D points in the viewing frustum. Our model requires patch-wise rendering of size (P, P) to formulate the collaborative contrastive loss. However, we can only render a patch less than 64×64 in each view due to GPU memory bottleneck (Garbin et al., 2021). Thus, it hardly covers a sufficient receptive field to capture the global context, using the pre-trained DINO. To solve this problem, we adopt a *Strided Ray Sampling* strategy (Schwarz et al., 2020b; Meng et al., 2021), to enlarge the receptive field of the patches while keeping computational cost fixed. Specifically, instead of sampling a patch of adjacent locations $P \times P$, we sample rays with an interval

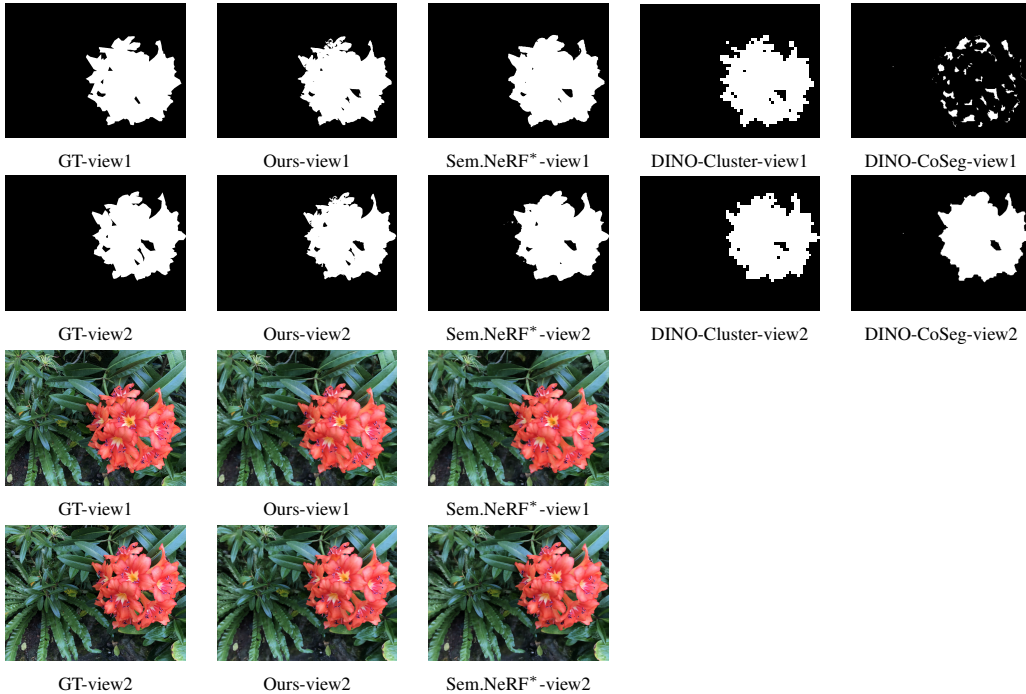


Figure 4: Qualitative results on scene *Flower*. In the last column, DINO-CoSeg mistakenly matches several discrete patches, as DINO has higher activation on just a few tokens on the foreground patches, which may lead to view-inconsistent and disconnected co-segmentation results. * superscript denotes the supervised method. DINO-Cluster and DINO-CoSeg are not able to perform novel view synthesis and thus we only show the co-segmentation results.

k , resulting in a receptive field of $(P \times k) \times (P \times k)$. Then, we optimize the overall pipeline using a balanced loss function:

$$\mathcal{L} = \lambda_0 \mathcal{L}_{\text{photometric}} + \lambda_1 \mathcal{L}_{\text{app}} + \lambda_2 \mathcal{L}_{\text{geo}}, \quad (11)$$

where λ_0 , λ_1 , and λ_2 are balancing weights.

4 EXPERIMENTS

4.1 EXPERIMENT SETUP

Datasets We evaluate all methods on three representative datasets: Local Light Field Fusion (LLFF) dataset (Mildenhall et al., 2019), Tank and Temples (T&T) dataset (Riegler & Koltun, 2020) and BlendedMVS (Yao et al., 2020). Particularly, we use the forward-facing scenes $\{Flower, Fortress\}$ from LLFF dataset, scene *Statue* with multiple objects from BlendedMVS dataset, and unbounded scene *Truck* from hand-held 360° captures large-scale scenes. We choose these representative scenes because they contain at least one common object among most views. We manually labeled all test views as a binary mask to provide a fair comparison for all methods and used them to train Semantic-NeRF. Foreground objects appearing in most views are labeled as 1, while others are labeled as 0. The camera poses of scene *Truck* are estimated by COLMAP SfM (Schonberger & Frahm, 2016) and are processed by NeRF++ (Zhang et al., 2020). We train our model on LLFF with resolution 1008×756 resolution, T&T with 980×546 , and BlendedMVS with 768×576 . Train and test splits follow NeRF (Mildenhall et al., 2020a) and NeRF++ (Zhang et al., 2020).

4.2 EXPERIMENT RESULTS

Training Details We first implement the collaborative contrastive loss upon the original NeRF model (Mildenhall et al., 2020a). In training, we first train NeRF-SOS without segmentation branch following the NeRF training recipe (Mildenhall et al., 2020b) for 150k iterations. Next, we load the weight and start to train the segmentation branch alone using the stride ray sampling for another 50k iterations. The loss weights λ_0 , λ_1 , λ_2 , λ_{id} , and λ_{neg} are set 0, 1, 0.01, 1 and 1 in training

Table 1: Quantitative evaluation of the novel view synthesis and object segmentation on scene *Flower*, with several 2D object discovery frameworks and the supervised Semantic-NeRF.

Scene " <i>Flower</i> "	PSNR \uparrow	SSIM \uparrow	LPIPS \downarrow	NV-ARI \uparrow	IoU(BG) \uparrow	IoU(FG) \uparrow	mIoU \uparrow
DINO+Cluster (Caron et al., 2021)	-	-	-	0.8951	0.9701	0.8933	0.9317
DOCS (Li et al., 2018)	-	-	-	0.0097	0.4824	0.2461	0.3643
DINO+CoSeg (Amir et al., 2021)	-	-	-	0.5946	0.9036	0.5961	0.7498
NeRF-SOS (Ours)	25.96	0.7717	0.1502	0.9529	0.9869	0.9503	0.9686
Semantic-NeRF (Zhi et al., 2021) (Supervised)	25.52	0.7500	0.1739	0.9104	0.9743	0.9090	0.9417

Table 2: Quantitative evaluation of the rendering quality and object segmentation on scene *Fortress*.

Scene " <i>Fortress</i> "	PSNR \uparrow	SSIM \uparrow	LPIPS \downarrow	NV-ARI \uparrow	IoU(BG) \uparrow	IoU(FG) \uparrow	mIoU \uparrow
DINO+Cluster (Caron et al., 2021)	-	-	-	0.4939	0.8200	0.5612	0.6905
DOCS (Li et al., 2018)	-	-	-	0.7412	0.9329	0.7265	0.8297
DINO+CoSeg (Amir et al., 2021)	-	-	-	0.9503	0.9886	0.9395	0.9640
NeRF-SOS (Ours)	29.78	0.8517	0.1079	0.9802	0.9955	0.9751	0.9853
Semantic-NeRF (Zhi et al., 2021) (Supervised)	29.78	0.8578	0.0906	0.9838	0.9963	0.9799	0.9881

the segmentation branch. The segmentation branch is formulated as a four-layer MLP with ReLU as the activation function. The dimensions of hidden layers and output layers are set as 256 and 2, respectively. The segmentation results are based on K-means clustering on the segmentation logits. We train semantic-NeRF (Zhi et al., 2021) 200k in total for fair comparisons. We randomly sample eight patches from different viewpoints (a.k.a batch size N is 8) in training. The patch size of each sample is set as 64×64 , with the patch stride as 6. We use the official pre-trained DINO-ViT in a self-supervised manner on ImageNet dataset as our 2D feature extractor. The pre-trained DINO backbone is kept frozen for all layers during training. All hyperparameters are carefully tuned by a grid search, and the best configuration is applied to all experiments. All models are trained on an NVIDIA RTX A6000 GPU with 48 GB memory.

Implementation of the Patch Selection We reconstruct positive and negative pairs on the fly during training. Given N rendered patches from N different viewpoints in training, we fed the patches into the DINO-ViT and obtained the [CLS] tokens. Next, we compute a $N \times N$ similarity matrix using the cosine similarity with the [CLS] tokens. The negative pairs are selected from the pair with the lowest similarity in each row; the positive pairs are set as the identity pairs. Overall, $2N$ pairs (N positives + N negatives) are formulated per iteration to compute the collaborative contrastive loss.

Metrics We adopt the Adjusted Rand Index (ARI) as our metric to evaluate the clustering quality. As we only consider the ARI in novel views, we report it as NV-ARI. We also adopt mean Intersection-over-Union to measure segmentation quality for both object and background, as we set the clusters with larger activation as foreground by DINO. To evaluate the rendering quality, we follow NeRF (Mildenhall et al., 2020a), adopting peak signal-to-noise ratio (PSNR), the structural similarity index measure (SSIM) (Wang et al., 2004) and learned perceptual image patch similarity (LPIPS) (Zhang et al., 2018) as evaluation metrics.

Self-supervised Object Segmentation on LLFF We build NeRF-SOS on the vanilla NeRF (Mildenhall et al., 2020a) to validate its effectiveness on LLFF datasets. Two groups of current object segmentation are adopted for comparisons: *i.* NeRF-based methods, including our NeRF-SOS, and supervised Semantic-NeRF (Zhi et al., 2021) trained with annotated masks; and *ii.* image-based object co-segmentation methods: DINO-CoSeg (Amir et al., 2021), DINO-ViT with K-means clustering (Caron et al., 2021), and DOCS (Li et al., 2018). As image-based co-segmentation methods cannot evaluate novel views, we pre-render the new views using NeRF and construct image pairs between the first image in the test set with others for DINO-CoSeg (Amir et al., 2021) and DOCS (Li et al., 2018). The evaluations on DINO-ViT (Caron et al., 2021) clustering also use the pre-rendered color images, obtaining its DINO feature in the last layer and performing K-means to identify clusters of data objects.

Quantitative comparisons against other segmentation methods are provided in Table 1 and Table 2, together with qualitative visualizations shown in Figure 4. Here, we visualize two distinct views to show segmentation consistency across views. These results convey several observations to us: **1).** NeRF-SOS consistently outperforms image-based co-segmentation in evaluation metrics and view-consistency. **2).** Compared with SoTA supervised NeRF segmentation method (Semantic-NeRF (Zhi et al., 2021)), our method effectively segments the object within the scene and performs on par in both evaluation metrics and visualization.

Self-supervised Object Segmentation on Unbounded Scene To test the generalization ability of the proposed collaborative contrastive loss, we implement it on NeRF++ (Zhang et al., 2020) to

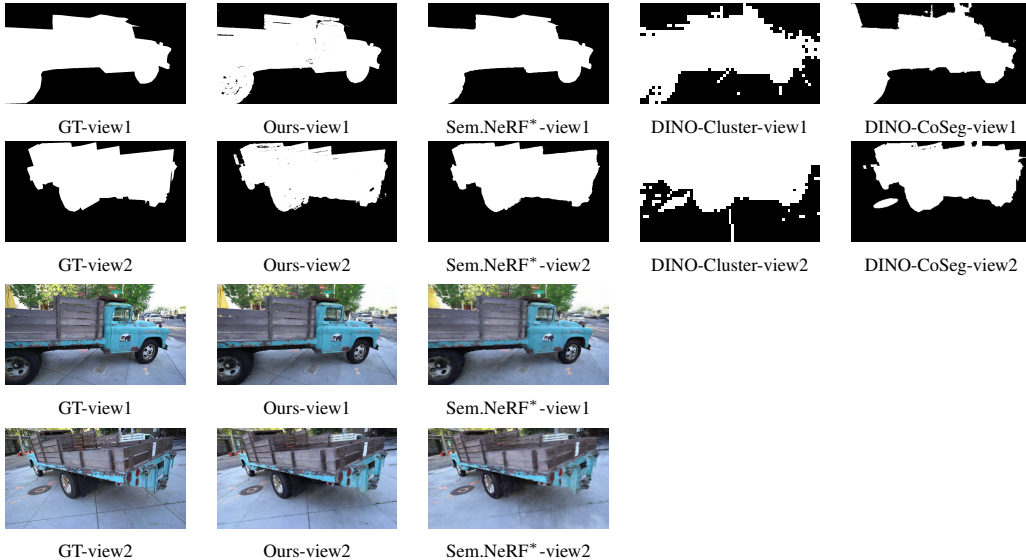


Figure 5: Novel view object segmentation results on unbounded scene *Truck*. NeRF-SOS (the 2nd column) produces view-consistent masks more than other self-supervised methods. It even generates finer details than supervised Semantic-NeRF++ (see the gaps between wooden slats in view1 and the side view mirror in view. 2). DINO-Cluster and DINO-CoSeg are not able to perform novel view synthesis and thus we only show the co-segmentation results.

Table 3: Quantitative results of the object segmentation results on outdoor unbounded scene *Truck*, with several 2D object discovery frameworks and the supervised Semantic-NeRF. We can see the self-supervised NeRF-SOS performs on par with the supervised methods.

Scene " <i>Truck</i> "	PSNR \uparrow	SSIM \uparrow	LPIPS \downarrow	NV-ARI \uparrow	IoU(BG) \uparrow	IoU(FG) \uparrow	mIoU \uparrow
DINO+Cluster (Caron et al., 2021)	-	-	-	0.2937	0.6239	0.6153	0.6196
DOCS (Li et al., 2018)	-	-	-	0.1517	0.6845	0.2463	0.4654
DINO+CoSeg (Amir et al., 2021)	-	-	-	0.8571	0.9408	0.9080	0.9244
NeRF-SOS (Ours)	22.20	0.7000	0.2691	0.9207	0.9689	0.9455	0.9572
Semantic-NeRF++ (Zhi et al., 2021) (Supervised)	21.08	0.6350	0.4114	0.9674	0.9869	0.9782	0.9826

test with a more challenging unbounded scene. Here, we mainly evaluate all previously mentioned methods on scene *Truck* as it is the only scene captured surrounding an object provided by NeRF++. We re-implement Semantic-NeRF using NeRF++ as the backbone model for unbounded setting, termed Semantic-NeRF++, following the training recipe of NeRF++. Qualitative and quantitative results are shown in Figure 5 and Table 3. We can see that NeRF-SOS still surpasses state-of-the-art image-based object co-segmentation methods. Compared with supervised Semantic-NeRF++, NeRF-SOS achieves slightly worse results in terms of quantitative metrics. Yet from the visualizations, we see that NeRF-SOS yields quite decent segmentation quality. For example, **1**). In Figure 5(Ours-view2), NeRF-SOS can recognize the side view mirror adjacent to the truck. **2**). In Figure 5(Ours-view1) NeRF-SOS can distinguish the apertures between the wooden slats as those apertures have distinct depths than the neighboring slats, thanks to the geometry-aware contrastive loss.

Impact of the Geometry Contrastive Loss To understand the impact of the geometry contrastive loss, we perform experiments on unbounded scene *Truck* and report results in Figure 6. In this part, we set two baseline models, either using appearance or geometric contrastive loss alone on NeRF++, as visual features and their geometry can all serve as cues for a better-distilled segmentation feature field. We can see that without geometric constraints (4th column), the segmentation branch failed to cluster spatially continuous objects; without visual cues (5th column), the model lost the perception of the central object. In contrast, a collaborative loss generates convincing object segmentation by considering scene appearance and geometry.

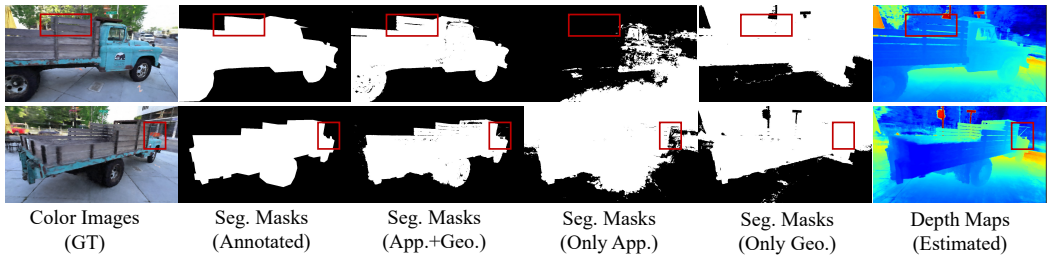


Figure 6: Object segmentation of three variants losses are shown in columns 3, 4, and 5: the collaborative loss (APP.+Geo.), appearance-only loss (App.); geometric-only loss (Geo.).

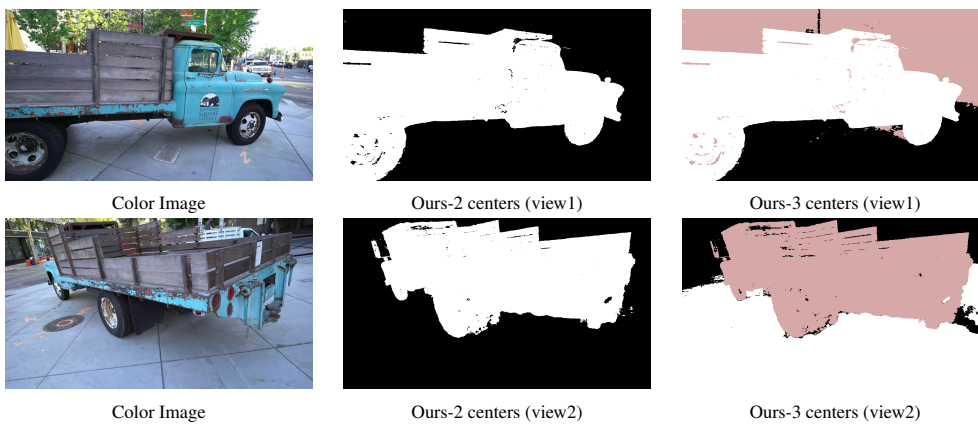


Figure 7: Qualitative results on scene *Truck* with different cluster centers on its distilled segmentation field. Note that the cross-view visualized colors of multiple-center clustering are not corresponding to the subject ID, as we perform unsupervised clustering.

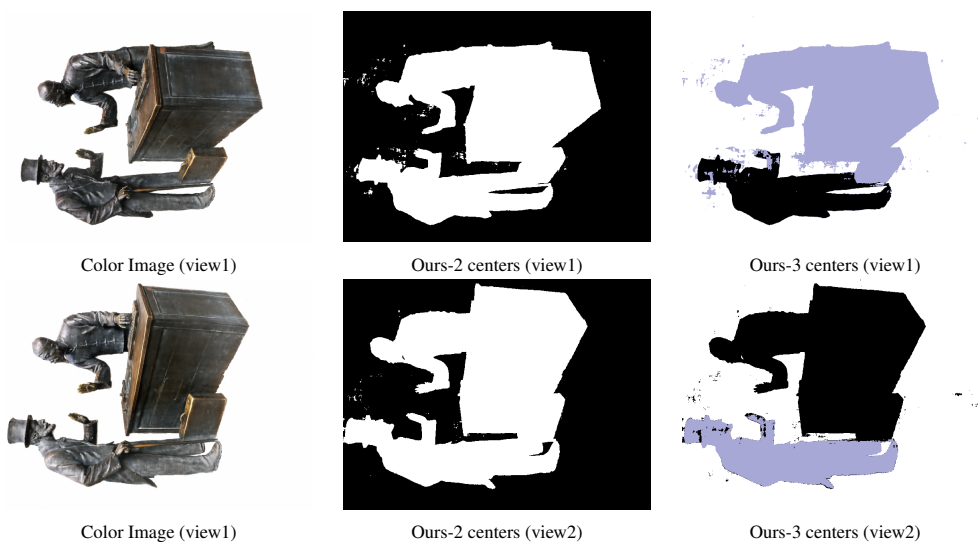


Figure 8: Qualitative results on scene *Statues* with different cluster centers on its distilled segmentation field.

4.3 QUALITATIVE RESULTS OF MORE CLUSTER CENTERS

We perform the study by performing multiple-center clusters on the distilled segmentation field in Figure 7. As can be seen, regions with distinct appearances and physical distances are separated into different clusters. Qualitative visualization on a subset of BlendedMVS (Yao et al., 2020) (scene *Statue*, pre-processing by NSVF (Liu et al., 2020b)) is provided in Figure 8. Here, we visualize two different views to show segmentation results, with the cluster number equaling 2 or 3.

5 CONCLUSION, DISCUSSION OF LIMITATION AND BROADER IMPACT

We present NeRF-SOS, a framework that learns object segmentation for any view from complex real-world scenes. A self-supervised framework, NeRF-SOS leverages a collaborative contrastive loss in appearance-segmentation and geometry-segmentation levels are included. Comprehensive experiments on forward-facing scenes and unbounded scenes are conducted, in comparison to SoTA image-based object segmentation frameworks and fully supervised Semantic-NeRF. NeRF-SOS consistently performs better than image-based methods, and sometimes generates finer segmentation details than its supervised counterparts. Similar to other scene-specific NeRF methods, one limitation of NeRF-SOS is that it cannot segment across scenes, which we will explore as future work. As for broader impact, this work for the first time attempts a self-supervised 3D object segmentation framework for complex real-world scenes using NeRF, which contributes meaningfully to reducing the annotation cost required by advanced 3D CV models.

REFERENCES

- Shir Amir, Yossi Gandelsman, Shai Bagon, and Tali Dekel. Deep vit features as dense visual descriptors. *arXiv preprint arXiv:2112.05814*, 2021.
- Jonathan T Barron, Ben Mildenhall, Matthew Tancik, Peter Hedman, Ricardo Martin-Brualla, and Pratul P Srinivasan. Mip-nerf: A multiscale representation for anti-aliasing neural radiance fields. In *IEEE International Conference on Computer Vision (ICCV)*, 2021.
- Mathilde Caron, Hugo Touvron, Ishan Misra, Hervé Jégou, Julien Mairal, Piotr Bojanowski, and Armand Joulin. Emerging properties in self-supervised vision transformers. In *Proceedings of the IEEE/CVF International Conference on Computer Vision*, pp. 9650–9660, 2021.
- Eric Chan, Marco Monteiro, Peter Kellnhofer, Jiajun Wu, and Gordon Wetzstein. pi-GAN: Periodic implicit generative adversarial networks for 3D-aware image synthesis. <https://arxiv.org/abs/2012.00926>, 2020.
- Ting Chen, Simon Kornblith, Mohammad Norouzi, and Geoffrey Hinton. A simple framework for contrastive learning of visual representations. In *International conference on machine learning*, pp. 1597–1607. PMLR, 2020.
- Xingyu Chen, Qi Zhang, Xiaoyu Li, Yue Chen, Feng Ying, Xuan Wang, and Jue Wang. Hallucinated neural radiance fields in the wild, 2021.
- Jang Hyun Cho, Utkarsh Mall, Kavita Bala, and Bharath Hariharan. Picie: Unsupervised semantic segmentation using invariance and equivariance in clustering. In *Proceedings of the IEEE/CVF Conference on Computer Vision and Pattern Recognition*, pp. 16794–16804, 2021.
- Joseph DeChicchis. Semantic understanding for augmented reality and its applications. 2020.
- Kangle Deng, Andrew Liu, Jun-Yan Zhu, and Deva Ramanan. Depth-supervised nerf: Fewer views and faster training for free. *arXiv preprint arXiv:2107.02791*, 2021.
- Robert A Drebin, Loren Carpenter, and Pat Hanrahan. Volume rendering. *ACM Siggraph Computer Graphics*, 22(4):65–74, 1988.
- Stephan J. Garbin, Marek Kowalski, Matthew Johnson, Jamie Shotton, and Julien Valentin. Fastnerf: High-fidelity neural rendering at 200fps. <https://arxiv.org/abs/2103.10380>, 2021.
- Mark Hamilton, Zhoutong Zhang, Bharath Hariharan, Noah Snavely, and William T Freeman. Unsupervised semantic segmentation by distilling feature correspondences. *arXiv preprint arXiv:2203.08414*, 2022.
- Kaiming He, Haoqi Fan, Yuxin Wu, Saining Xie, and Ross Girshick. Momentum contrast for unsupervised visual representation learning. In *Proceedings of the IEEE/CVF conference on computer vision and pattern recognition*, pp. 9729–9738, 2020.
- Olivier J Hénaff, Skanda Koppula, Evan Shelhamer, Daniel Zoran, Andrew Jaegle, Andrew Zisserman, João Carreira, and Relja Arandjelović. Object discovery and representation networks. *arXiv preprint arXiv:2203.08777*, 2022.
- Geoffrey Hinton, Oriol Vinyals, Jeff Dean, et al. Distilling the knowledge in a neural network. *arXiv preprint arXiv:1503.02531*, 2(7), 2015.
- Jyh-Jing Hwang, Stella X Yu, Jianbo Shi, Maxwell D Collins, Tien-Ju Yang, Xiao Zhang, and Liang-Chieh Chen. Segsort: Segmentation by discriminative sorting of segments. In *Proceedings of the IEEE/CVF International Conference on Computer Vision*, pp. 7334–7344, 2019.
- Wonbong Jang and Lourdes Agapito. Codenerf: Disentangled neural radiance fields for object categories. In *Proceedings of the IEEE/CVF International Conference on Computer Vision*, pp. 12949–12958, 2021.
- Xu Ji, Joao F Henriques, and Andrea Vedaldi. Invariant information clustering for unsupervised image classification and segmentation. In *Proceedings of the IEEE/CVF International Conference on Computer Vision*, pp. 9865–9874, 2019.

- Zhang Jiakai, Liu Xinhang, Ye Xinyi, Zhao Fuqiang, Zhang Yanshun, Wu Minye, Zhang Yingliang, Xu Lan, and Yu Jingyi. Editable free-viewpoint video using a layered neural representation. In *ACM SIGGRAPH*, 2021.
- Mohammad Mahdi Johari, Yann Lepoittevin, and François Fleuret. Geonerf: Generalizing nerf with geometry priors. *arXiv preprint arXiv:2111.13539*, 2021.
- Sosuke Kobayashi, Eiichi Matsumoto, and Vincent Sitzmann. Decomposing nerf for editing via feature field distillation. *arXiv preprint arXiv:2205.15585*, 2022.
- Adarsh Kowdle, Dhruv Batra, Wen-Chao Chen, and Tsuhan Chen. imodel: interactive co-segmentation for object of interest 3d modeling. In *European Conference on Computer Vision*, pp. 211–224. Springer, 2010.
- Weihaio Li, Omid Hosseini Jafari, and Carsten Rother. Deep object co-segmentation. In *Asian Conference on Computer Vision*, pp. 638–653. Springer, 2018.
- Yunfan Li, Peng Hu, Zitao Liu, Dezhong Peng, Joey Tianyi Zhou, and Xi Peng. Contrastive clustering. In *2021 AAAI Conference on Artificial Intelligence (AAAI)*, 2021.
- David Lindell, Julien Martel, and Gordon Wetzstein. AutoInt: Automatic integration for fast neural volume rendering. <https://arxiv.org/abs/2012.01714>, 2020.
- Lingjie Liu, Jiatao Gu, Kyaw Zaw Lin, Tat-Seng Chua, and Christian Theobalt. Neural sparse voxel fields. In *Advances in Neural Information Processing Systems (NeurIPS)*, volume 33, 2020a.
- Lingjie Liu, Jiatao Gu, Kyaw Zaw Lin, Tat-Seng Chua, and Christian Theobalt. Neural sparse voxel fields. *Advances in Neural Information Processing Systems*, 33:15651–15663, 2020b.
- Steven Liu, Xiuming Zhang, Zhoutong Zhang, Richard Zhang, Jun-Yan Zhu, and Bryan Russell. Editing conditional radiance fields, 2021.
- Stephen Lombardi, Tomas Simon, Gabriel Schwartz, Michael Zollhoefer, Yaser Sheikh, and Jason Saragih. Mixture of volumetric primitives for efficient neural rendering, 2021.
- Ricardo Martin-Brualla, Noha Radwan, Mehdi Sajjadi, Jonathan T. Barron, Alexey Dosovitskiy, and Daniel Duckworth. NeRF in the wild: Neural radiance fields for unconstrained photo collections. <https://arxiv.org/abs/2008.02268>, 2020.
- Nelson Max. Optical models for direct volume rendering. *IEEE Transactions on Visualization and Computer Graphics (TVCG)*, 1995.
- Quan Meng, Anpei Chen, Haimin Luo, Minye Wu, Hao Su, Lan Xu, Xuming He, and Jingyi Yu. Gnerf: Gan-based neural radiance field without posed camera. In *Proceedings of the IEEE/CVF International Conference on Computer Vision*, pp. 6351–6361, 2021.
- Ben Mildenhall, Pratul P Srinivasan, Rodrigo Ortiz-Cayon, Nima Khademi Kalantari, Ravi Ramamoorthi, Ren Ng, and Abhishek Kar. Local light field fusion: Practical view synthesis with prescriptive sampling guidelines. *ACM Transactions on Graphics (TOG)*, 2019.
- Ben Mildenhall, Pratul P Srinivasan, Matthew Tancik, Jonathan T Barron, Ravi Ramamoorthi, and Ren Ng. Nerf: Representing scenes as neural radiance fields for view synthesis. In *European conference on computer vision*, pp. 405–421. Springer, 2020a.
- Ben Mildenhall, Pratul P Srinivasan, Matthew Tancik, Jonathan T Barron, Ravi Ramamoorthi, and Ren Ng. Nerf: Representing scenes as neural radiance fields for view synthesis. In *European conference on computer vision*, pp. 405–421. Springer, 2020b.
- Daniel Rebaín, Wei Jiang, Soroosh Yazdani, Ke Li, Kwang Moo Yi, and Andrea Tagliasacchi. DeRF: Decomposed radiance fields. <https://arxiv.org/abs/2011.12490>, 2020.
- Christian Reiser, Songyou Peng, Yiyi Liao, and Andreas Geiger. Kilonerf: Speeding up neural radiance fields with thousands of tiny mlps. In *IEEE International Conference on Computer Vision (ICCV)*, 2021.

- Gernot Riegler and Vladlen Koltun. Free view synthesis. In *European Conference on Computer Vision (ECCV)*, 2020.
- Carsten Rother, Tom Minka, Andrew Blake, and Vladimir Kolmogorov. Cosegmentation of image pairs by histogram matching-incorporating a global constraint into mrfs. In *2006 IEEE Computer Society Conference on Computer Vision and Pattern Recognition (CVPR'06)*, volume 1, pp. 993–1000. IEEE, 2006.
- Pedro Savarese, Sunnie SY Kim, Michael Maire, Greg Shakhnarovich, and David McAllester. Information-theoretic segmentation by inpainting error maximization. In *Proceedings of the IEEE/CVF Conference on Computer Vision and Pattern Recognition*, pp. 4029–4039, 2021.
- Johannes L Schonberger and Jan-Michael Frahm. Structure-from-motion revisited. In *Proceedings of the IEEE conference on computer vision and pattern recognition*, pp. 4104–4113, 2016.
- Katja Schwarz, Yiyi Liao, Michael Niemeyer, and Andreas Geiger. Graf: Generative radiance fields for 3D-aware image synthesis. In *Advances in Neural Information Processing Systems (NeurIPS)*, volume 33, 2020a.
- Katja Schwarz, Yiyi Liao, Michael Niemeyer, and Andreas Geiger. Graf: Generative radiance fields for 3d-aware image synthesis. *Advances in Neural Information Processing Systems*, 33: 20154–20166, 2020b.
- Tong Shen, Guosheng Lin, Lingqiao Liu, Chunhua Shen, and Ian Reid. Weakly supervised semantic segmentation based on co-segmentation. In *BMVC*, 2017.
- Oriane Siméoni, Gilles Puy, Huy V Vo, Simon Roburin, Spyros Gidaris, Andrei Bursuc, Patrick Pérez, Renaud Marlet, and Jean Ponce. Localizing objects with self-supervised transformers and no labels. *arXiv preprint arXiv:2109.14279*, 2021.
- Karl Stelzner, Kristian Kersting, and Adam R Kosiorok. Decomposing 3d scenes into objects via unsupervised volume segmentation. *arXiv preprint arXiv:2104.01148*, 2021.
- Cheng Sun, Min Sun, and Hwann-Tzong Chen. Direct voxel grid optimization: Super-fast convergence for radiance fields reconstruction. *arXiv preprint arXiv:2111.11215*, 2021.
- Matthew Tancik, Pratul P Srinivasan, Ben Mildenhall, Sara Fridovich-Keil, Nithin Raghavan, Utkarsh Singhal, Ravi Ramamoorthi, Jonathan T Barron, and Ren Ng. Fourier features let networks learn high frequency functions in low dimensional domains. In *Advances in Neural Information Processing Systems (NeurIPS)*, 2020.
- Zachary Teed and Jia Deng. Raft: Recurrent all-pairs field transforms for optical flow. In *European conference on computer vision*, pp. 402–419. Springer, 2020.
- Alex Trevithick and Bo Yang. GRF: Learning a general radiance field for 3D scene representation and rendering. <https://arxiv.org/abs/2010.04595>, 2020.
- Narek Tumanyan, Omer Bar-Tal, Shai Bagon, and Tali Dekel. Splicing vit features for semantic appearance transfer. *arXiv preprint arXiv:2201.00424*, 2022.
- Wouter Van Gansbeke, Simon Vandenhende, Stamatios Georgoulis, Marc Proesmans, and Luc Van Gool. Scan: Learning to classify images without labels. In *European Conference on Computer Vision*, pp. 268–285. Springer, 2020.
- Wouter Van Gansbeke, Simon Vandenhende, Stamatios Georgoulis, and Luc Van Gool. Unsupervised semantic segmentation by contrasting object mask proposals. In *Proceedings of the IEEE/CVF International Conference on Computer Vision*, pp. 10052–10062, 2021.
- Sara Vicente, Carsten Rother, and Vladimir Kolmogorov. Object cosegmentation. In *CVPR 2011*, pp. 2217–2224. IEEE, 2011.
- Suhani Vora, Noha Radwan, Klaus Greff, Henning Meyer, Kyle Genova, Mehdi SM Sajjadi, Etienne Pot, Andrea Tagliasacchi, and Daniel Duckworth. Nesf: Neural semantic fields for generalizable semantic segmentation of 3d scenes. *arXiv preprint arXiv:2111.13260*, 2021.

- Can Wang, Menglei Chai, Mingming He, Dongdong Chen, and Jing Liao. Clip-nerf: Text-and-image driven manipulation of neural radiance fields. *arXiv preprint arXiv:2112.05139*, 2021a.
- Qianqian Wang, Zhicheng Wang, Kyle Genova, Pratul P Srinivasan, Howard Zhou, Jonathan T Barron, Ricardo Martin-Brualla, Noah Snavely, and Thomas Funkhouser. Ibrnet: Learning multi-view image-based rendering. In *IEEE Conference on Computer Vision and Pattern Recognition (CVPR)*, 2021b.
- Zhou Wang, Alan C Bovik, Hamid R Sheikh, and Eero P Simoncelli. Image quality assessment: from error visibility to structural similarity. *IEEE transactions on image processing*, 13(4):600–612, 2004.
- Bangbang Yang, Yinda Zhang, Yinghao Xu, Yijin Li, Han Zhou, Hujun Bao, Guofeng Zhang, and Zhaopeng Cui. Learning object-compositional neural radiance field for editable scene rendering. In *Proceedings of the IEEE/CVF International Conference on Computer Vision*, pp. 13779–13788, 2021.
- Yao Yao, Zixin Luo, Shiwei Li, Jingyang Zhang, Yufan Ren, Lei Zhou, Tian Fang, and Long Quan. Blendedmvs: A large-scale dataset for generalized multi-view stereo networks. In *Proceedings of the IEEE/CVF Conference on Computer Vision and Pattern Recognition*, pp. 1790–1799, 2020.
- Alex Yu, Ruilong Li, Matthew Tancik, Hao Li, Ren Ng, and Angjoo Kanazawa. Plenotrees for real-time rendering of neural radiance fields. In *IEEE International Conference on Computer Vision (ICCV)*, 2021a.
- Alex Yu, Vickie Ye, Matthew Tancik, and Angjoo Kanazawa. pixelnerf: Neural radiance fields from one or few images. In *IEEE Conference on Computer Vision and Pattern Recognition (CVPR)*, 2021b.
- Hong-Xing Yu, Leonidas J Guibas, and Jiajun Wu. Unsupervised discovery of object radiance fields. *arXiv preprint arXiv:2107.07905*, 2021c.
- Kai Zhang, Gernot Riegler, Noah Snavely, and Vladlen Koltun. Nerf++: Analyzing and improving neural radiance fields. *arXiv preprint arXiv:2010.07492*, 2020.
- Richard Zhang, Phillip Isola, Alexei A Efros, Eli Shechtman, and Oliver Wang. The unreasonable effectiveness of deep features as a perceptual metric. In *Proceedings of the IEEE conference on computer vision and pattern recognition*, pp. 586–595, 2018.
- Hengshuang Zhao, Li Jiang, Jiaya Jia, Philip HS Torr, and Vladlen Koltun. Point transformer. In *Proceedings of the IEEE/CVF International Conference on Computer Vision*, pp. 16259–16268, 2021.
- Shuaifeng Zhi, Tristan Laidlow, Stefan Leutenegger, and Andrew J Davison. In-place scene labelling and understanding with implicit scene representation. In *Proceedings of the IEEE/CVF International Conference on Computer Vision*, pp. 15838–15847, 2021.